Original Article

Aspirin impedes non-small cell lung cancer development via fine-tuning the CD36 localization regulated by GPIHBP1

Wei Liu[1#], Dujuan Qiao[2#], Jia Chen[3], Ya Gao[1], Katsuhiro Okuda[4], Yoshihisa Shimada[5], Linong Yao[1]

[1]Department of Critical Care Medicine, Tangdu Hospital of Air Force Military Medical University, Xi'an, China; [2]Department of Anesthesiology & Perioperative Medicine (D), Xi'an People's Hospital (Xi'an Fourth Hospital), Xi'an, China; [3]The College of Life Sciences, Northwest University, Xi'an, China; [4]Department of Thoracic and Pediatric Surgery, Nagoya City University Graduate School of Medical Sciences, Nagoya, Japan; [5]Department of Thoracic Surgery, Tokyo Medical University, Tokyo, Japan

Contributions: (I) Conception and design: L Yao; (II) Administrative support: L Yao; (III) Provision of study materials or patients: W Liu; (IV) Collection and assembly of data: D Qiao, W Liu; (V) Data analysis and interpretation: J Chen, Y Gao, K Okuda, Y Shimada; (VI) Manuscript writing: All authors; (VII) Final approval of manuscript: All authors.

[#]These authors contributed equally to this work.

Correspondence to: Linong Yao, MD, PhD. Department of Critical Care Medicine, Tangdu Hospital of Air Force Military Medical University, No. 569 Xinsi Road, Baqiao District, Xi'an 710034, China. Email: yaolin@fmmu.edu.cn.

Background: Lung cancer, a commonly diagnosed malignancy, is the leading cause of cancer-related death worldwide. Aspirin suppresses the progression and metastasis of various cancers. However, the effect of aspirin on non-small cell lung cancer (NSCLC) has not been fully understood. It has been established that glycosylphosphatidylinositol HDL-binding protein 1 (GPIHBP1) and CD36 play a vital role in lipid metabolism and transport. This study aimed to clarify the mechanism by which aspirin inhibits NSCLC cell proliferation and metastasis via GPIHBP1.

Methods: The blood and tissues of 10 patients with NSCLC treated with aspirin and 10 patients without aspirin were collected and analyzed via RNA sequencing. GPIHBP1 expression was determined by immunohistochemistry (IHC), Western blotting, and quantitative real time polymerase chain reaction (qRT-PCR). A series of functional experiments were performed to evaluate the effects of aspirin on NSCLC progression in a GPIHBP1-dependent manner. The potential mechanism of GPIHBP1 was explored via coimmunoprecipitation and immunofluorescence staining. The effect of GPIHBP1 on tumor growth and metastasis was verified by constructing subcutaneous xenograft tumor model in nude mice.

Results: GPIHBP1 was downregulated and was increased by treatment with aspirin in lung cancer tissues. Furthermore, GPIHBP1 overexpression inhibited the migration, cell proliferation, and epithelial-mesenchymal transition process in NSCLC cells while promoting their apoptosis, while in cells with GPIHBP1 knockdown, the opposite was observed. Mechanistically, GPIHBP1 directly interacted with CD36 while GPIHBP1 knockdown disrupted CD36 localization, thus promoting tumor progression and metastasis in NSCLC cells. In addition, through *in vivo* xenograft experiments, we found that GPIHBP1 overexpression inhibited tumor growth and metastasis.

Conclusions: Our findings provide new insights into the mechanism by which aspirin suppresses lung cancer development in a GPIHBP1-dependent manner and may provide a promising target in NSCLC treatment.

Keywords: Aspirin; glycosylphosphatidylinositol HDL-binding protein 1 (GPIHBP1); non-small cell lung cancer (NSCLC); proliferation; metastasis

Submitted Dec 03, 2024. Accepted for publication Feb 19, 2025. Published online Feb 27, 2025.
doi: 10.21037/tlcr-2024-1174
View this article at: https://dx.doi.org/10.21037/tlcr-2024-1174

Introduction

Despite advances in treatment over the last few decades, lung cancer remains the leading cause of cancer-related morbidity and mortality (1). Lung cancer can be divided into small cell lung cancer and non-small cell lung cancer (NSCLC) according to histology, with NSCLC accounting for approximately 80% of all lung cancers (2,3). Over the past decade, although many advances have been achieved in the treatment of lung cancer, the prognosis of patients with advanced stage NSCLC remains highly unsatisfactory. Lung cancer's susceptibility to metastasis and recurrence are chiefly responsible for poor prognosis of patients (4). Therefore, it is critical to elucidate the underlying mechanisms of lung cancer metastasis and to identify the related molecular markers in order to facilitate the early detection and diagnosis of lung cancer in patients.

Aspirin, a classic nonsteroidal anti-inflammatory drug (NSAID), is widely used for prevention and treatment of cardiovascular and cerebrovascular diseases (5). Numerous studies have confirmed the association between long-term aspirin use and a lower risk of cancer mortality, especially in gastrointestinal cancers (6-8). Research has also demonstrated that aspirin can act directly on tumor cells and inhibit their metabolism, proliferation, drug resistance, and metastasis. A recent study revealed that aspirin can induce apoptosis in tumor cells and that its synergistic effect with erlotinib could induce apoptosis in human *EGFR*-mutated NSCLC cell lines (9). Another study reported that aspirin could induce an endoplasmic reticulum stress response by inhibiting GRP78 activity to inhibit the migration and invasion of NSCLC cells (10). And Liu *et al.* reported that Aspirin-triggered resolving D1 inhibits TGF-β1-induced epithelial-mesenchymal transition (EMT) through the inhibition of the mTOR pathway by reducing the expression of PKM2 in A549 lung cancer cells (11). Therefore, aspirin appears capable of mitigating NSCLC initiation and progression; however, the underlying molecular mechanisms by which aspirin exerts these effects are not completely understood.

Glycosylphosphatidylinositol HDL-binding protein 1 (GPIHBP1) is a longevity-related protein that crosses endothelial cells, where it reaches the abdominal plasma membrane and may capture lipoprotein lipase (LPL) and transport it to the lumen of the capillaries (12). When GPIHBP1 is defective, LPL is trapped in the gap and cannot reach the lumen of the capillaries, severely impairing triglyceride lipoprotein (TRL) processing, resulting in severe hypertriglyceridemia (13). In peripheral tissues, the intravascular processing of TRLs by GPIHBP1-LPL complexes is critical for the production of lipid nutrients in adjacent parenchymal cells (14). Pulmonary capillaries have high levels of GPIHBP1, which may play an important role in the clearing of LPL (15). CD36, a multiligand class B scavenger receptor, was reported to be involved in regulating lipid metabolism, and several studies have suggested that CD36 is upregulated and promotes tumor progression in various cancers (16,17). However, the role of GPIHBP1 in NSCLC is not well understood, and the exact nature of the interaction between GPIHBP1 and CD36 and the subsequent effect on NSCLC have not been extensively investigated.

We thus conducted this study to determine the effects of aspirin on the cell viability and migration of A549 and H1299 cells. We identified differentially expressed microRNAs (miRNAs) in exosomes from the plasma of patients NSCLC treated with or without aspirin using RNA sequencing and bioinformatic analyses. GPIHBP1 was found to be a potential biomarker in lung cancer. Furthermore, cells were transfected with overexpression or knockdown plasmid of GPIHBP1 to ascertain whether GPIHBP1 is involved in aspirin-induced tumor suppression.

Highlight box

Key findings

- Aspirin inhibits cell proliferation and migration in non-small cell lung cancer (NSCLC) cells. Patients with a low expression of glycosylphosphatidylinositol HDL-binding protein 1 (GPIHBP1) had a poor prognosis. GPIHBP1 inhibited the migration, cell proliferation, and epithelial-mesenchymal transition (EMT) process of NSCLC cell while promoting their apoptosis. GPIHBP1 directly interacts with CD36 and regulates the localization of CD36.

What is known and what is new?

- Aspirin can reduce the risk of a variety of cancers including digestive system tumors, breast cancer, and urinary system tumors. However, the underlying mechanism by which aspirin exerts its antitumor effects in NSCLC has not been fully explored.
- In this study, we demonstrated, for the first time, that GPIHBP1 was downregulated in lung cancer tissues but could be promoted by aspirin. The inhibitory effects of aspirin on tumor progression were impaired by GPIHBP1 knockdown. Specifically, GPIHBP1 interacted with CD36 and stabilized CD36 on the plasma membrane.

What is the implication, and what should change now?

- Our findings indicate that aspirin can inhibit lung cancer progression and metastasis in a GPIHBP1-dependent manner *in vitro* and *in vivo*. Aspirin and targeting of GPIHBP1 could serve as a promising therapeutic approach in NSCLC treatment.

Table 1 All siRNA sequences

siRNA	Sense	Antisense
Control-siRNA	TTCTCCGAACGTGTCACGT	ACGTGACACGTTCGGAGAA
GPIHBP1-siRNA	GACCTGCACAACCCTCATT	AGTCCAGCCTGTGCAATGT
CD36-siRNA	AAACACACAGGGATTCCTTTCAGATT	AAATCTGAAAGGAATCCCTGTGT

siRNA, small interfering RNA.

It was observed that the induction of GPIHBP1 was necessary for multiple suppressive effects of aspirin on tumor, including the hindering of cell viability, migration, epithelial-mesenchymal transition (EMT), and metastasis, as well as the promotion of apoptosis. Notably, we discovered that GPIHBP1 interacted with CD36, stabilizing CD36 on the plasma membrane to maintain normal cell viability and migration. Taken together, our study provides a novel understanding that aspirin could inhibit lung cancer progression and metastasis in a GPIHBP1-dependent manner, which may be a viable strategy for NSCLC treatment. And our results indicate that GPIHBP1 may be a potential biomarker or therapeutic target in NSCLC. We present this article in accordance with the ARRIVE and MDAR reporting checklists (available at https://tlcr.amegroups.com/article/view/10.21037/tlcr-2024-1174/rc).

Methods

Cell culture, plasmid transfection, and small-interfering RNA assay

Human NSCLC cell lines H1299 and A549 cells were obtained from the Cell Bank of Type Culture Collection of the Chinese Academy of Sciences (Shanghai, China). The cells were cultured in RPMI-1640 medium (MACGENE Biotechnology, Beijing, China) at 37 ℃ in a humidified incubator with 5% CO_2, supplemented with 1% penicillin/streptomycin sulfate (Solarbio, Beijing, China) and 10% fetal bovine serum (Gibco, USA).

To achieve overexpression GPIHBP1, lentiviral particles containing human full-length GPIHBP1 were prepared by OBiO Technology Corp., Ltd. (Shanghai, China) and were used to infect H1299 cells and A549 cells. Cells were transinfected with the lentiviral particles and were selected with puromycin (1 mg/mL) (Invitrogen, Thermo Fisher Scientific, Waltham, MA, USA) for 3 weeks to produce stably transfected cells. Western blotting and quantitative real time polymerase chain reaction (qRT-PCR) were used to evaluate the overexpression efficiency.

For the knockdown experiment, cells were treated with GPIHBP1 small interfering RNA (GPIHBP1-siRNA), CD36-siRNA, or control-siRNA. These siRNAs were provided by GenePharma (Shanghai, China). Subsequently, 2×10^5 cells per well were plated into a six-well plate, treated with siRNA (1–2 μg) for 12 h via Lipofectamine 3000 transfection reagent (cat. no. L3000015, Invitrogen), and then received the indicated treatment. Western blotting and qRT-PCR were used to evaluate the knockdown efficiency after 48 h of transfection. The sequences are listed in *Table 1*.

Patient samples

All experiments with human blood and tissue samples were collected at Tangdu Hospital (Xi'an, China) from July 2020 to December 2020. Written informed consents were obtained from each patient. The study protocol was performed in full accordance with the principles of the Declaration of Helsinki (as revised in 2013) and was approved by the Ethical Review Board of Tangdu Hospital (No. K202104-09). All tumor and adjacent normal lung tissues were confirmed by histological examination. The specimens were snap-frozen in liquid nitrogen and stored at −80 ℃. The tissue specimens were also fixed in 10% formalin and embedded for subsequent experimentation.

Exosomal RNA isolation and RNA-sequencing analysis

Exosomal RNA from plasma samples were extracted with the Direct-zol RNA kit (Zymo Research, Irvine, CA, USA) according to the manufacturers protocol. Exosomal RNA was sent to Genechem Co., Ltd. (Shanghai, China) for messenger RNA (mRNA) sequencing. Differential gene expression analysis was completed using the "limma" R package version 3.44.3 (The R Foundation for Statistical Computing) as previously reported (18). The fold change (FC) of each gene was log2 transformed and further analyzed using the R package "clusterProfiler" version 3.16.1.

Table 2 All primers sequences in RT-qPCRs

Gene	Forward	Reverse
GPIHBP1	GCAACCTGACGCAGAACTG	CCAGGGTGGGACATTGCAC
β-actin	GGCGGCACCACCATGTACCCT	AGGGGCCGGACTCGTCATACT
PKNOX2	GCAGGACTTCTGAGGCTTTCT	CACATGGAGGACTGTTCGGG
ADGRD1	CCCAGGAACATCCAGGCTTT	ATTGTGGGAGAGAGGCACAG
CRTAC1	AACTCAGTGCTGGAGATCC	AGAATCCTTGGCCACACTC
ST6GALNAC6	ATTTGACGACCTCTTCCGGG	TCTTGTTGCCCACATCAGCT
FAM83D	GCCTTCTACCAGGGCGCCTAC	ACGTCCATGACCACTGCAATCAC
MACROD2	TTGGCTCTGCTCTTCCATTT	GCCAAGAATCACCATGAGGT
CD36	TCACTGCGACATGATTAATGGTAC	ACGTCGGATTCAAATACAGCATAGAT

RT-qPCRs, reverse transcription polymerase chain reactions.

Table 3 Summary of 6 datasets of non-small cell lung cancer

ID	Dataset	Platform	Samples	Disease
1	GSE30219	GPL570	272 patients	NSCLC
2	GSE37745	GPL570	196 patients	NSCLC
3	GSE31210	GPL570	226 patients	LUAD
4	TCGA LUAD	Illumina	497 patients and 58 controls	LUAD
5	TCGA LUSC	Illumina	489 patients and 49 controls	LUSC
6	Exosome	Illumina	10 treated with aspirin and 10 controls	Lung cancer

LUAD, lung adenocarcinoma; LUSC, lung squamous cell carcinoma; NSCLC, non-small lung cancer cell.

RNA extraction and qRT-PCR

Total RNA from cells and tissue samples were isolated according to the TRIzol extraction method, and reverse transcription was performed using the HiFair III 1st Strand cDNA Synthesis SuperMix (Yeasen Biotechnology, Shanghai, China). qRT-PCR was carried out using Hieff qPCR SYBR Green Master Mix from (Yeasen Biotechnology). The primers were purchased from Tsingke Biotechnology (Shanghai, China). FCs of gene expression were calculated as $2^{-\Delta\Delta Ct}$. β-actin was used as an internal control for normalization. The primers involved in this experiment article are listed in *Table 2*.

Data download and preprocessing

GSE30219, GSE37745, and GSE31210 data were downloaded with the R software package from the Gene Expression Omnibus (GEO) database (https://www.ncbi.nlm.nih.gov/geo/). Fragments per kilobase per million mapped fragments data and somatic mutation data were obtained from UCSC Xena. The lung adenocarcinoma (LUAD) and lung squamous cell carcinoma (LUSC) datasets in The Cancer Genome Atlas (TCGA) were also examined in this study (*Table 3*). Gene expression matrix of the data was constructed via the "hgu133 plus2.db" package. Differential expression analysis in exosome derived from the plasma of patients in aspirin-applied and unapplied group was performed by using the edgeR package of R software. Gene Ontology (GO) function and Kyoto Encyclopedia of Genes and Genomes (KEGG) pathway enrichment analyses were used to identify the function of aspirin. Differentially expressed genes [DEGs; false-discovery rate (FDR) <0.05 and $|\log_2 FC| > 1$] were visualized and intersected with the GEO and TCGA data.

Immunohistochemistry (IHC), immunofluorescence (IF), and hematoxylin-eosin (HE) staining

For IHC and HE staining, the tissues in formalin-

fixed paraffin sections were sliced to a 5-μm thickness. IHC staining was performed using a universal two-step detection kit (ZSGB-Bio, Beijing, China) according to the manufacturer's instructions. The expression of each protein was semiquantitatively evaluated using a previously described method (19). Anti-GPIHBP1 (1:60; cat. no. ab224728; Abcam, Cambridge, UK) primary antibodies were used in this experiment. Images were obtained with a microscope (Nikon, Tokyo, Japan). HE staining was performed to determine the degree of metastasis in tissue samples in a manner previously described (20). Images were captured with a microscope (Nikon). The tumor area was quantified using ImageJ software (US National Institutes of Health, Bethesda, MD, USA).

For immunofluorescence (IF) staining, cells were fixed with 4% paraformaldehyde for 10 min, permeabilized in 0.4% Triton X-100 for 10 min, and blocked with 5% bovine serum albumin (BSA) in phosphate-buffered saline (PBS) for 1 h. The cells were incubated with anti-GPIHBP1 antibody (1:100; cat no. ab224728; Abcam) and anti-CD36 antibody (1:100; cat. no. 66395-1-lg; Proteintech Group, Rosemont, IL, USA) overnight at 4 ℃. After being washed three times with PBS, the cells were incubated with a goat anti-rabbit IgG secondary antibody conjugated with Alexa Fluor 488 (1:200; cat. no. A-11008; Thermo Fisher Scientific) and a goat anti-mouse IgG secondary antibody conjugated with Cy3 (1:200; cat. no. SA00009-1; Proteintech) for 1 h at room temperature. The nuclei were stained with DAPI (1:1,000; cat. no. C1005; Beyotime, Nantong, China). Images were obtained with a confocal laser scanning microscope (Nikon).

Cell counting kit-8 assay (CCK-8)

CCK-8 assay (Solarbio, Beijing, China) was used to assess cell proliferation. Cells were seeded in 96-well plates at a density of 4×10^3 cells per well overnight and treated with or without different concentrations of aspirin for the different times indicated. A solution of 20 μL of CCK-8 per well was added. After incubation at 37 ℃ for 2 h, 96-well plates were shocked for 15 s, and the solution was absorbed at 490 nm using enzyme-linked immunosorbent assay reader (Bio-Rad, Hercules, CA, USA).

Transwell assay

Cells in 300 μL of serum-free medium were added to the upper chambers at a density of 2×10^5 cells per well, and 500 μL of complete medium was added to the lower chambers. After 24 h of incubation, cells in the upper chambers were removed, and the filter was fixed and stained with 0.5% (w/v) crystal violet solution. Four randomly selected fields in each membrane were photographed under a C-5060 light microscope (Olympus, Tokyo, Japan). The migrated cells in randomly selected fields were analyzed with ImageJ software.

Western blotting

Cells were harvested and lysed in radioimmunoprecipitation (RIPA) lysis buffer (Beyotime) with 1 mM of phenylmethylsulfonyl fluoride (PMSF) (Solarbio) for 10 min on ice. Cell lysates were centrifuged for 15 min at 12,000 ×g at 4 ℃, supernatant was extracted, and protein concentrations were determined using a bicinchoninic acid (BCA) protein assay kit (Tiangen, Beijing, China). A total of 20–40 μg of protein per sample was separated via sodium dodecyl sulfate-polyacrylamide gel electrophoresis (SDS-PAGE) and transferred onto polyvinylidene fluoride (PVDF) membranes. After blocking in 0.1% Tris-buffered saline with Tween20 (TBST) with 5% fat-free milk for 1 h at room temperature, the membranes were incubated with primary antibodies at 4 ℃ overnight. After incubation with a secondary anti-mouse antibody (1:5,000; cat. no. SA00001-1; Proteintech) or anti-rabbit antibody (1:500; cat. no. SA00001-2; Proteintech) at room temperature for 1 h, the membranes were visualized with enhanced chemiluminescence (ECL) substrate (cat. no. 34096; Thermo Fisher Scientific) and scanned with a ChemiDoc XRS system (Bio-Rad). Densitometric analyses of the immunoblots were performed using ImageJ software.

The following primary antibodies were used in this study: anti-GPIHBP1 antibody (1:1,000; cat. no. ab224728; Abcam), anti-CD36 antibody (1:1,000; cat. no. 66395-1-Ig; Proteintech), anti-E-cadherin (1:1,000; cat. no. 60335-1-Ig; Proteintech), anti-N-cadherin (1:1,000; cat. no. 22018-1-AP; Proteintech), anti-vimentin (1:1,000; cat. no. 22031-1-AP; Proteintech), anti-MMP9 (1:1,000; cat. no. 27306-1-AP; Proteintech), anti-β-actin [1:1,000; cat. no. 3700; Cell Signaling Technology (CST), Danvers, MA, USA], and anti-ATP1A1 (1:1,000; cat. no. 11802-1-AP; Proteintech).

Co-immunoprecipitation

In brief, NSCLC cells were washed with ice-cold PBS three times and lysed with immunoprecipitation lysis buffer

(25 mM Tris-HCl pH 7.4, 150 mM NaCl, 1% NP-40, 1 mM EDTA, and 5% glycerol; cat. no. 87787; Thermo Fisher Scientific) supplemented with a protease and phosphatase inhibitor cocktail (cat. no. 5872; CST). The lysates were incubated with 1 µg of antibodies for immunoprecipitation at 4 ℃ overnight. Protein A/G magnetic beads were added for 3 h at 4 ℃. After the beads were washed with immunoprecipitation lysis buffer three times, the protein samples containing dithiothreitol were heated and separated by electrophoresis. After being transferred to PVDF membranes, the proteins were immunoblotted with anti-GPIHBP1 and anti-CD36 antibodies. Finally, 40 µL of cell lysates were saved for use as positive controls and loading controls in immunodetection.

Cell fractionation

Plasma membrane protein and cytosol protein were extracted with the Mem-PER Plus Membrane Protein Extraction Kit (cat. no. 89842; Thermo Fisher Scientific) for Western blotting according to the manufacturer's protocols. Briefly, 5×10^6 cells were washed twice with cell wash solution via centrifugation at 300 ×g for 5 min at 4 ℃. Subsequently, the pellet was homogenized in permeabilization buffer for 10 min at 4 ℃. The permeabilized cells were centrifuged for 15 min at 1,600 ×g. The supernatant contained cytosolic proteins. The pellet was resuspended and incubated in solubilization buffer for 30 min at 4 ℃. The tubes were centrifuged at 16,000 ×g for 15 min at 4 ℃. The supernatant contained plasma membrane protein. The cytosolic and membrane fractions were stored at –80 ℃ until further analyses.

Determination of apoptosis via flow cytometry

The apoptosis rate *in vitro* was determined via flow cytometry analysis with an Annexin V-FITC/propidium iodide (PI) apoptosis detection kit (cat. no. C1062S; Beyotime) according to the manufacturer's instructions. The composition of apoptotic cells was analyzed by flow cytometry.

Xenograft model

The protocol for animal experimentation in this study was approved by the Ethics Committee on Animal Experiments of Air Force Military Medical University (No. IACUC-20231251). All the animal experiments were carried out in accordance with the Guide for the Care and Use of Laboratory Animals (8^{th} edition) published by the US National Institutes of Health. A protocol was prepared before the study without registration. Briefly, 6-week-old male BALB/c athymic nude mice were purchased from Beijing Weitonglihua Co., Ltd. and were maintained in a chamber with constant humidity of 55%±2% and a temperature of 22±2 ℃ for a cycle of 12-h light and 12-h dark in specific pathogen-free (SPF) conditions. Each nude mouse was subcutaneously injected with 1×10^7 A549 cells. Tumor volume was recorded every 5 days to assess tumor growth. The volume of the xenograft tumor was determined by the following standard formula: length × width × width × 0.5. Lung tumor was monitored and evaluated with the IVIS spectrum *in vivo* imaging system (PerkinElmer, Waltham, MA, USA) 30 days postinjection. Tumor weight was also recorded 30 days postinjection. At the end of the experiment, all mice were killed. The tumor and lung tissues were collected for further analysis.

Statistical analysis

All of the assays were performed at least three times independently. Statistical analyses were performed using GraphPad Prism 8 (GraphPad Software, La Jolla, CA, USA). Data are presented as the mean ± standard deviation (SD). Statistical significance was assessed with the Student *t*-test for experiments with two groups or one-way analysis of variance (ANOVA) followed by the Tukey multiple comparisons test for experiments with more than two groups. The significance of differences between different time points or concentrations was evaluated using one-way ANOVA followed by the Dunnett multiple comparisons test. The survival rate data of lung cancer patients were downloaded from the Kaplan-Meier plotter online tool (http://www.kmplot.com) and were analyzed by Kaplan-Meier analysis with the log-rank test. Continuous variables were summarized as means ± SD, and categorical variables as frequencies and percentages. Baseline characteristics between patients with aspirin– and aspirin+ were compared using the *t*-test for continuous variables and chi-square test or fisher's exact test for categorical variables if appropriate, respectively. $P<0.05$ was considered statistically significant.

Results

Aspirin perturbed gene expression associated with survival in patients with NSCLC

Although aspirin has been reported to suppress the cell proliferation in NSCLC (21), the underlying mechanism and related targets have not been fully elucidated. Recently, many studies have shown that exosomal miRNAs and proteins are a critical component of tumor metastasis (22-24). We first extracted exosomes from the plasma of patients with NSCLC treated with or without aspirin. As shown in Table S1, there was no difference in the background characteristics between the two cohorts. We then performed RNA sequencing and analyzed the differentially expressed miRNAs from exosomes (*Figure 1A*). RNA-sequencing analysis showed that aspirin influenced the expression of 5,685 genes, including 3,367 upregulated genes and 2,318 downregulated genes ($|\log_2 FC| \geq 1.0$ and FDR <0.05; *Figure 1A* and Figure S1). Moreover, GO function and KEGG pathway enrichment analysis indicated that aspirin modulated cellular process, biological regulation, metabolic process, catalytic activity, etc., suggesting that aspirin has widespread effects on NSCLC cells (*Figure 1B,1C*).

To examine the effect of aspirin on LUAD cell proliferation and migration, both H1299 and A549 cells were first treated with different concentrations of aspirin for different durations to optimize the condition of aspirin treatment. As shown in *Figure 1D,1E*, aspirin reduced cell proliferation as detected by CCK-8 assay in a dose- and time-dependent manner in both A549 and H1299 cells. Furthermore, the results of cell migration analysis conducted by Transwell assay indicated that aspirin inhibited the cell migration of both A549 and H1299 cells (*Figure 1F,1G*). Taken together, these results suggest that aspirin attenuated cell proliferation and migration in NSCLC.

GPIHBP1 was positively correlated with prognosis in patients with NSCLC

We conducted differential expression analysis of TCGA database (*Table 3*). The R package "limma" was used to conduct matrix differential expression analysis, and 1,744 genes (740 upregulated and 1,004 downregulated) in the LUAD dataset and 3,053 genes (with 1,458 upregulated and 1,595 downregulated) in the LUSC dataset ($|\log_2 FC| > 1$ and FDR <0.05) were extracted (*Figure 2A,2B*). The intersection of the three data sets (LUAD in TCGA, LUSC in TCGA, and plasma-derived exosomes analysis) yielded 277 DEGs (*Figure 2C*). These DEGS were then screened in TCGA dataset for univariate Cox proportional hazard regression analysis. This yielded 126 genes with significant prognostic ability in LUAD and 48 genes in LUSC. Analysis was conducted by using the R "survival" and "survminer" packages in the high- or low-expression groups. Subsequently, 113 genes with log rank P<0.05 were selected as independent prognostic indicators. This was followed by intersection with the plasma-derived exosome analysis data, and 7 NSCLC prognostic markers (PKNOX2, GPIHBP1, ADGRD1, CRTAC1, ST6GALNAC6, FAM83D, and MACROD2) were obtained. Survival analysis was then performed to test the applicability of the prognostic markers in LUAD. The area under the curve (AUC) of LUAD at 1 year indicated that the prognostic risk score performed well on the prediction of survival (Figure S2). Considering that the increase in mRNA level of GPIHBP1 was the most significant among these genes, we selected GPIHBP1 for subsequent analysis (Figure S3). GPIHBP1 exhibited a significant difference in expression profiles between tumor and normal tissues according the pancancer databases TNMplot and Gene Expression Profiling Interactive Analysis (GEPIA) (*Figure 2D,2E*) and was associated with prolonged survival time (P<0.001; *Figure 2F*). In addition, the protein levels of GPIHBP1 in tissues from operation were assessed via Western blotting. The results indicated that compared with adjacent normal lung tissue (ANT), GPIHBP1 in lung tumor tissue (T) was significantly decreased (*Figure 2G,2H*). Representative IHC experiments demonstrated similar results (*Figure 2I*). Overall, the above results suggest that lower GPIHBP1 expression was associated with poorer prognosis in lung cancer.

GPIHBP1 inhibited NSCLC progression in vitro

To further determine the critical function of GPIHBP1 in NSCLC progression, we manipulated the expression of GPIHBP1 in NSCLC cells. As shown in Figure S4A-S4F, the protein and mRNA levels of GPIHBP1 were successfully knocked down via transfection with siRNA and were significantly overexpressed by transfection with recombinant lentivirus in A549 or H1299 cells, respectively. First, the upregulated protein and mRNA levels of GPIHBP1 were observed in aspirin-treated NSCLC cells (*Figure 3A-3C*). Importantly, GPIHBP1 overexpression decreased migration (*Figure 3D,3E*) and cell proliferation

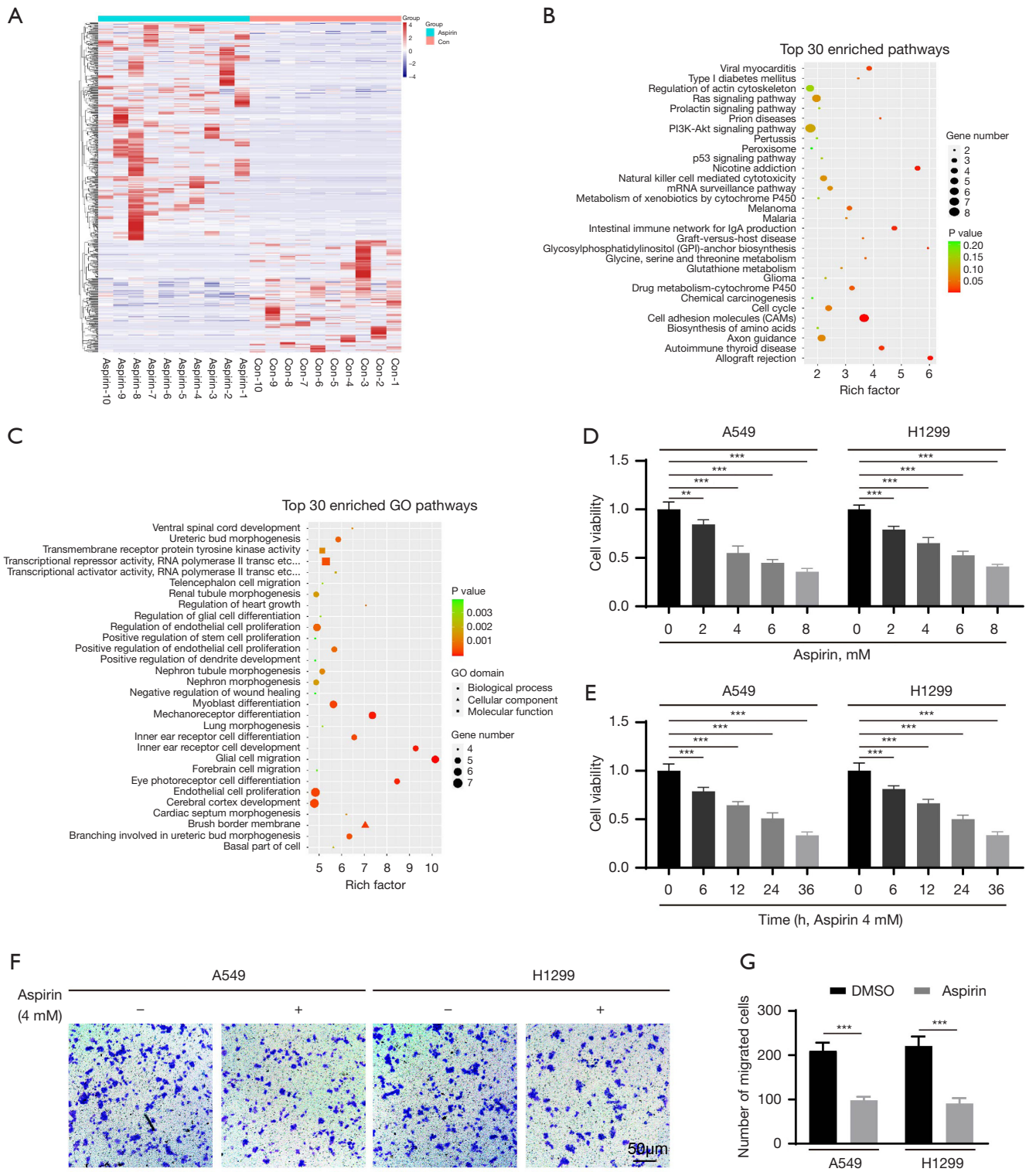

Figure 1 Aspirin inhibited cell proliferation and migration in NSCLC cells. (A) Heatmap of the differentially expressed miRNAs in the plasma of 10 patients with NSCLC treated without aspirin and 10 patients with NSCLC treated with aspirin. Red represents high gene expression, and blue represents low gene expression. The color brightness of each band reflects the difference in multiples. (B,C) KEGG

analysis and GO enrichment analysis were performed to identify the differentially expressed miRNAs involved in biological pathways. (D,E) Effects of aspirin on cell proliferation was detected by CCK-8 assay. A549 and H1299 cells were (D) treated with indicated concentration of aspirin for 24 h or (E) 4-mM of aspirin at the indicated time (n=4/group). (F,G) Cell migration detected by Transwell assay. Cells were treated with 4 mM of aspirin for 24 h. The staining method for Transwell assay was crystal violet staining. Images were taken under light microscopy (scale bar: 50 μm). The numbers of migration cells in seven randomly selected fields were counted (n=4/group). Data are shown as the mean ± standard deviation. **, P<0.01; ***, P<0.001. CCK-8, cell counting kit 8; DMSO, dimethyl sulfoxide; GO, Gene Ontology; KEGG, Kyoto Encyclopedia of Genes and Genomes; miRNA, microRNA; NSCLC, non-small cell lung cancer.

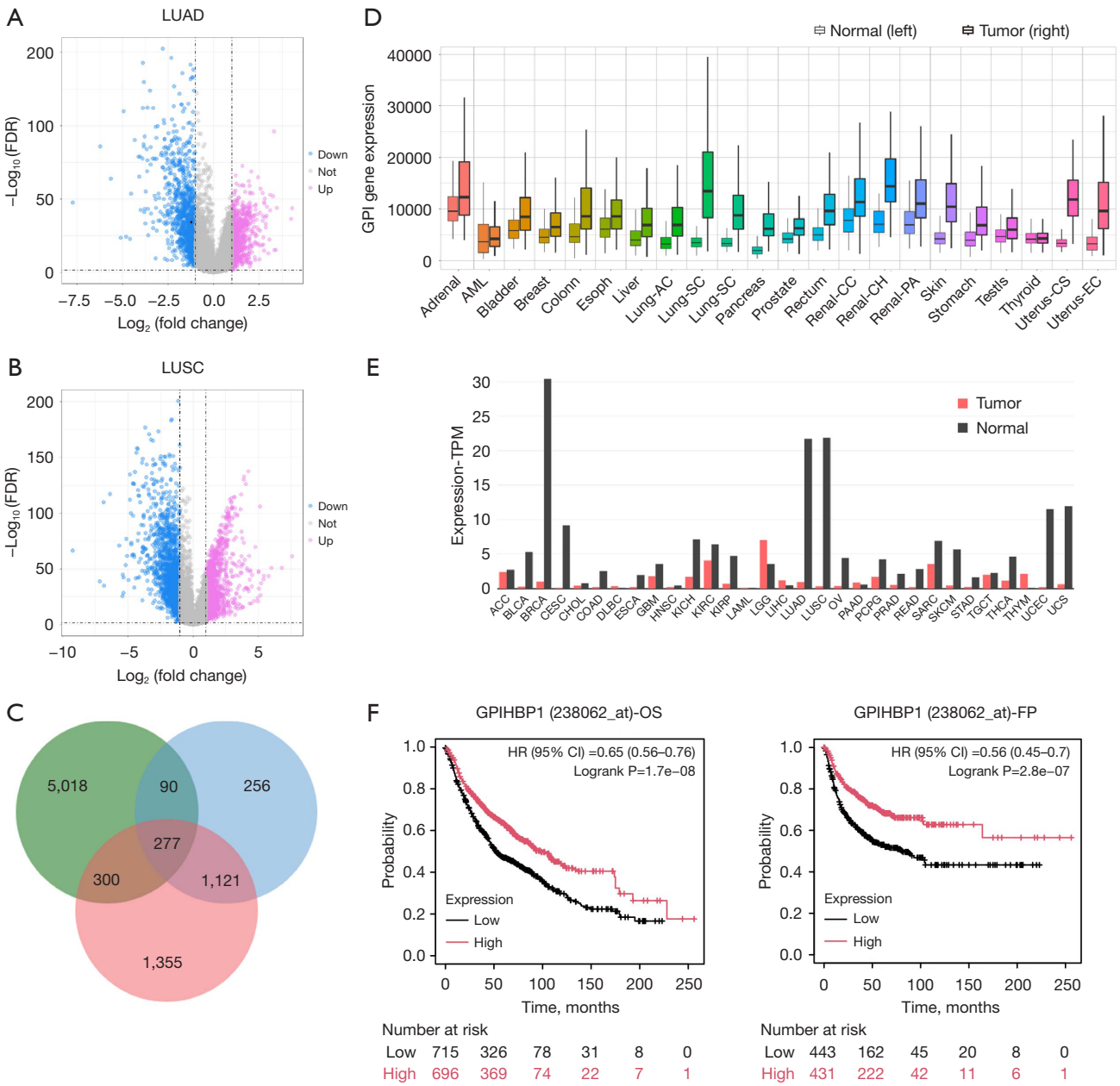

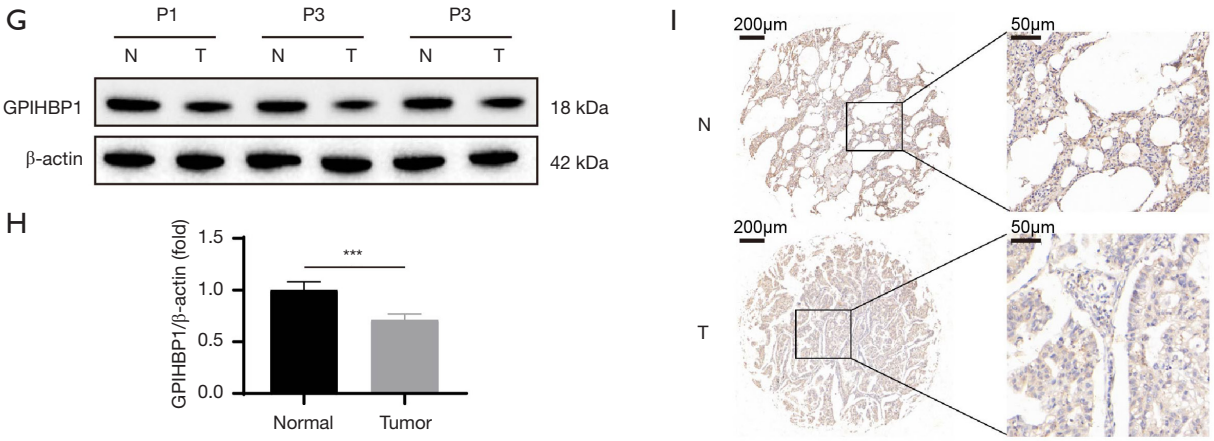

Figure 2 Integrated identification and enrichment analysis of GPIHBP1 obtained from the datasets. (A,B) Volcano plot for DEGs in the (A) LUAD and (B) LUSC dataset. Upregulated genes are represented by red dots; downregulated genes are represented by blue dots. (C) The Venn diagram of DEGs. (D,E) Expression profiles of GPIHBP1 in pancancer from (D) TNMplot and (E) GEPIA. (F) The OS (left) and FP (right) of GPIHBP1 in lung cancer are analyzed using the Kaplan-Meier plotter. (G,H) Western blotting and quantification of GPIHBP1 expression in ANT (N) or lung tumor tissue (T) in patients with NSCLC (n=5/group). (I) IHC staining analysis of GPIHBP1 protein levels in ANT (N) or lung tumor tissue (T) in patients with NSCLC. Scale bar (left), 200 μm. Scale bar (right), 50 μm. Data are shown as the mean ± standard deviation. ***, P<0.001. ANT, adjacent normal lung tissue; CI, confidential interval; DEGs, differentially expressed genes; FDR, false-discovery rate; FP, first progression survival; GEPIA, Gene Expression Profiling Interactive Analysis; GPIHBP1, glycosylphosphatidylinositol HDL-binding protein 1; HR, hazard ratio; IHC, immunohistochemistry; LUAD, lung adenocarcinoma; LUSC, lung squamous cell carcinoma; NSCLC, non-small cell lung cancer; OS, overall survival; TPM, transcripts per million.

(*Figure 3F*) while increasing the proportion of apoptotic cells (*Figure 3G,3H*) in both A549 and H1299 cells. In contrast, migration and cell proliferation were increased in GPIHBP1-knockdown cells while cell apoptosis was reduced (*Figure 3A-3H*). More importantly, at the molecular level of EMT, E-cadherin significantly elevated while N-cadherin, vimentin, and MMP-9 levels were significantly inhibited in cells overexpressing GPIHBP1, while the opposite was observed in cells with GPIHBP1 knockdown (*Figure 3I-3L*). Collectively, these data indicated that GPIHBP1 inhibited the migration, cell proliferation, and EMT of NSCLC cells while promoting their apoptosis.

Aspirin inhibited lung cancer progression by increasing GPIHBP1 expression

To examine whether aspirin inhibits proliferation and metastasis of NSCLC cells via regulating GPIHBP1 expression, we treated NSCLC cells with overexpression or knockdown of GPIHBP1 with 4 mM of aspirin for 24 h. Transwell assays and CCK-8 assays results revealed that compared to corresponding controls, GPIHBP1-overexpressed NSCLC cells underwent a greater degree of cell migration and proliferation suppression via aspirin treatment, while the positive effects of aspirin on cell apoptosis were further strengthened (*Figure 4A-4E*). Moreover, in GPIHBP1-overexpressed NSCLC cells, upregulation of E-cadherin by treatment with aspirin and downregulation of N-cadherin, vimentin, and MMP-9 by treatment with aspirin were more pronounced (*Figure 4F-4I*). Our results also showed that aspirin decreased migration, cell proliferation, and EMT while increasing cell apoptosis, which was largely attenuated by GPIHBP1 knockdown in both A549 cells and H1299 cells (*Figure 4A-4I*). Therefore, we can conclude that the inhibitory effects of aspirin on tumor progression were impaired in GPIHBP1-knockdown NSCLC cells.

GPIHBP1 stabilized CD36 on the plasma membrane in vitro

Given the important roles of GPIHBP1 in inhibiting the tumor progression in lung cancer, we next investigated the underlying molecular mechanism responsible for the regulation of GPIHBP1-mediated migration, cell proliferation, apoptosis, and EMT. It has been reported

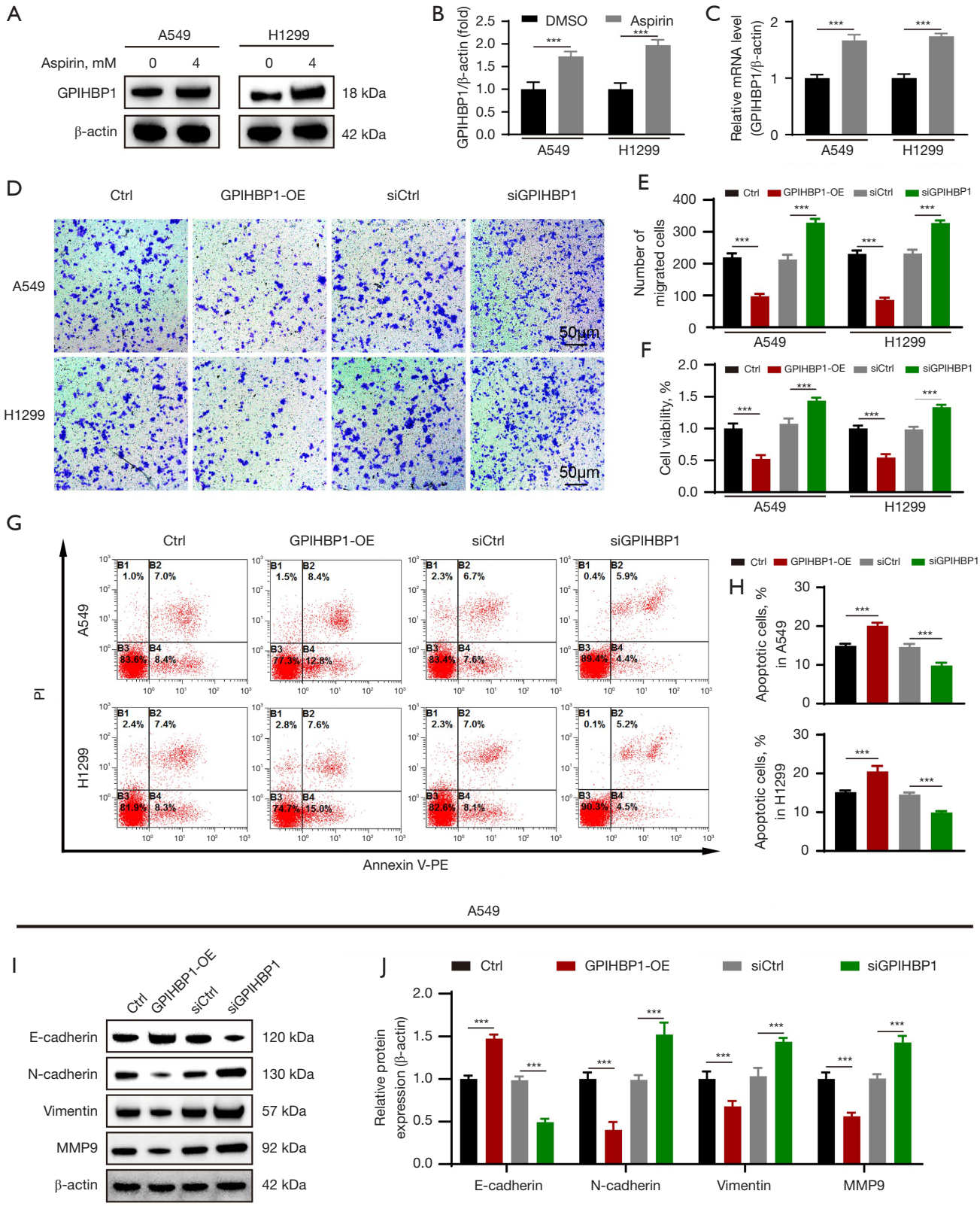

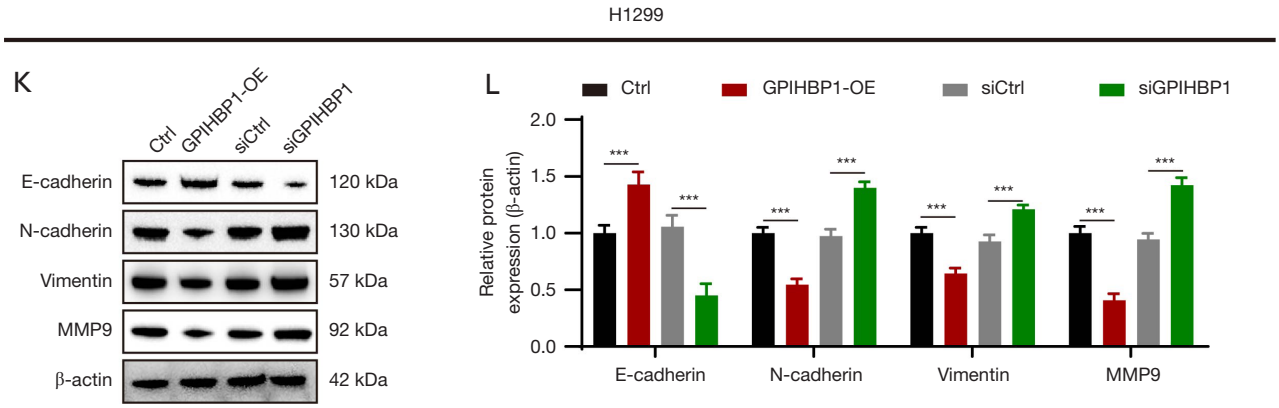

Figure 3 Upregulation of GPIHBP1 inhibited migration, proliferation, and EMT while enhancing apoptosis *in vitro*. (A,B) Western blotting and quantification of GPIHBP1 expression in A549 cells or H1299 cells treated with DMSO or aspirin (4 mM) treatment for 24 h (n=4/group). (C) qRT-PCR of GPIHBP1 mRNA levels in A549 cells or H1299 cells treated with DMSO or aspirin (4 mM) treatment for 24 h (n=4/group). (D-L) The GPIHBP1 protein was overexpressed by constructed lentiviral transfection and knocked down by small interfering RNA in NSCLC cells. Cells were collected for determination of migration detected by (D,E) Transwell assay, cell proliferation detected by (F) CCK-8 assay, and apoptosis by (G,H) annexin V-FITC/propidium iodide (PI) staining. Images were taken under light microscopy (scale bar: 50 μm). The staining method for Transwell assay was crystal violet staining. Protein expression of E-cadherin, N-cadherin, vimentin, and MMP-9 was determined by Western blotting with density quantitative analysis (I-L) (n=4/group). Data are shown as the mean ± standard deviation. ***, P<0.001. CCK-8, cell counting kit 8; DMSO, dimethyl sulfoxide; EMT, epithelial-mesenchymal transition; GPIHBP1, glycosylphosphatidylinositol HDL-binding protein 1; MMP-9, matrix metalloproteinase-9; NSCLC, non-small cell lung cancer; OE, overexpression; qRT-PCR, quantitative real time polymerase chain reaction.

that GPIHBP1 plays an important role in regulating lipid metabolism in a variety of tumor types (25). CD36 has also been demonstrated to regulate lipid metabolism and tumor progression in lung cancer cells (26). In our study, we first detected the proteins and mRNA levels of CD36 in lung cancer cells with or without aspirin treatment. The total proteins and mRNA levels of CD36 were not affected by aspirin treatment (Figure S5A-S5C). Moreover, Co-immunoprecipitation analysis confirmed that GPIHBP1 interacted endogenously with CD36 in whole-cell lysates and plasma membrane lysates in both A549 or H1299 cells (*Figure 5A-5E*). Moreover, the IF experiment also indicated that CD36 colocalized with GPIHBP1 (*Figure 5C,5F*). Considering that GPIHBP1 knockdown does not significantly affect total CD36 expression, we next investigated whether GPIHBP1 regulates the translocation of CD36 from the plasma membrane to the cytoplasm. Interestingly, we found that GPIHBP1 knockdown in NSCLC cells significantly promoted the translocation of CD36 from plasma membrane into the cytoplasm, indicated by the decreased expression of CD36 in plasma membrane lysates and the increased expression of cytosolic lysates (*Figure 5G-5J*). Taken together, our findings suggest that although GPIHBP1 does not affect the expression of CD36, it interacts with CD36 to stabilize its translocation on plasma membrane.

The procancer effect of GPIHBP1knockdown was abolished by CD36 knockdown

To determine whether the role of GPIHBP1 is related to CD36 levels, the NSCLC cells infected with siGPIHBP1 were also subjected to si-CD36 to block CD36 expression. As shown in Figure S6A-S6C, the protein and mRNA levels of CD36 were successfully knocked down by transfection with siRNA. As expected, CD36 knockdown significantly decreased migration (*Figure 6A,6B*), cell proliferation (*Figure 6C*), and EMT (*Figure 6D-6G*) while increasing the proportion of apoptotic cells (*Figure 6H,6I*) in both A549 and H1299 cells. Importantly, all the aggravating effects of GPIHBP1 knockdown on tumor progression were blocked by CD36 knockdown (*Figure 6A-6I*). Compared with NSCLC cells with GPIHBP1 knockdown, NSCLC cells with both GPIHBP1 and CD36 knockdown exhibited significantly decreased migration (*Figure 6A,6B*), cell proliferation (*Figure 6C*), and EMT (*Figure 6D-6G*) but

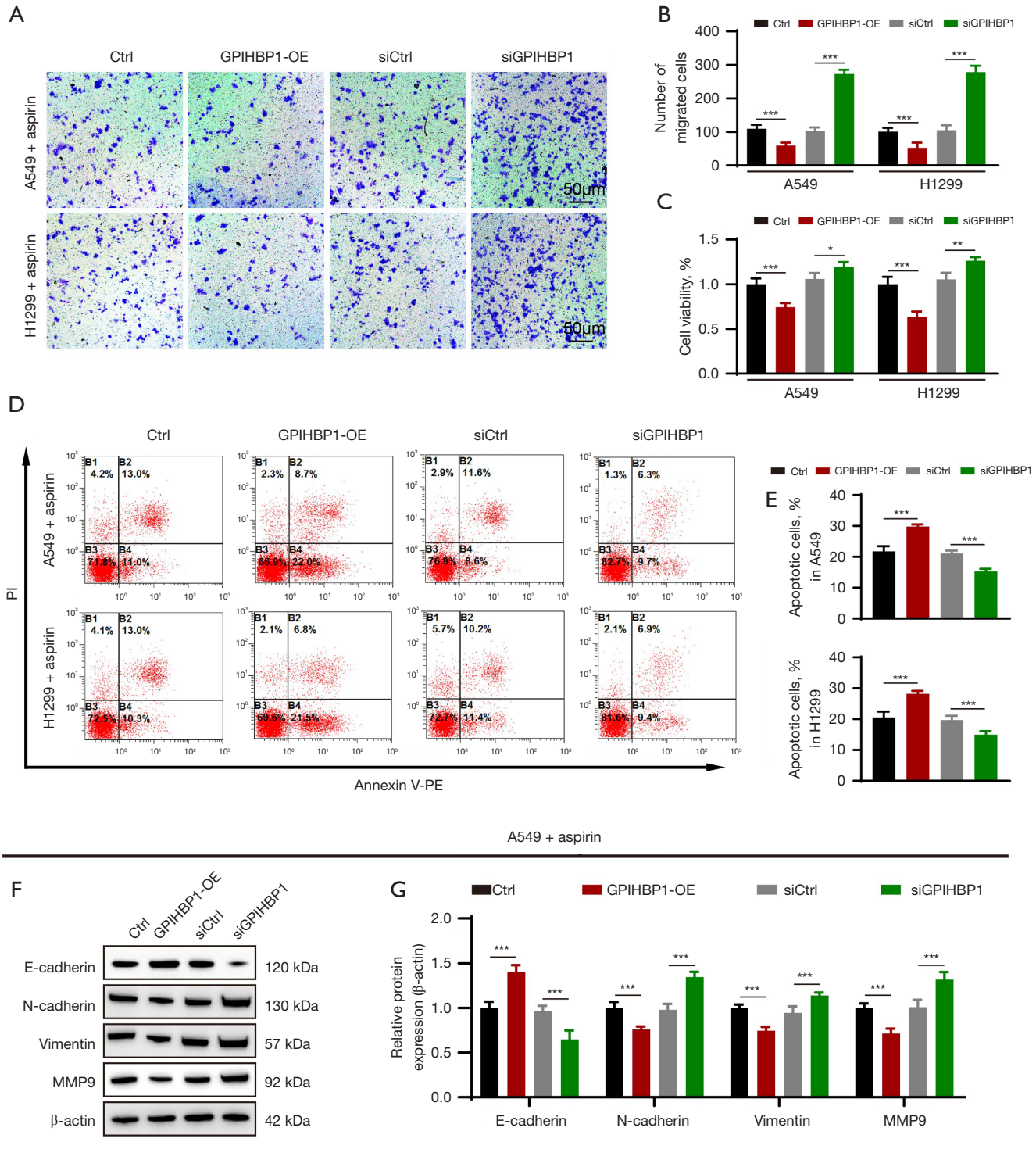
A
Ctrl
GPIHBP1-OE
siCtrl
siGPIHBP1
A549 + aspirin
H1299 + aspirin
50μm
B
Number of migrated cells
A549
H1299
C
Cell viability, %
D
PI
Annexin V-PE
E
Apoptotic cells, % in A549
Apoptotic cells, % in H1299
A549 + aspirin
F
E-cadherin
N-cadherin
Vimentin
MMP9
β-actin
120 kDa
130 kDa
57 kDa
92 kDa
42 kDa
G
Relative protein expression (β-actin)

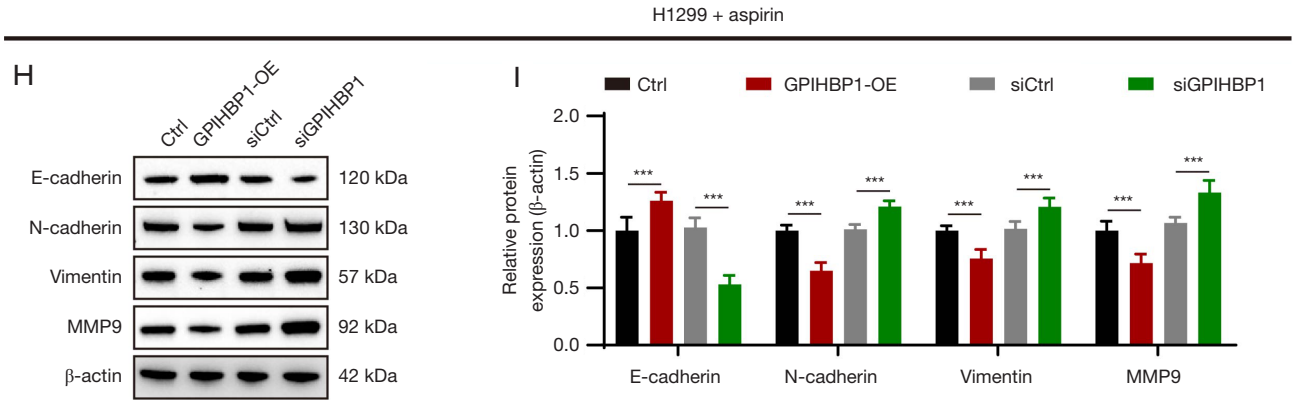

Figure 4 The effects of aspirin on cell proliferation, migration, EMT, and apoptosis were associated with GPIHBP1 expression. (A-I) In NSCLC cells, the GPIHBP1 protein was overexpressed via lentiviral transfection or knocked down by small interfering RNA and followed aspirin (4 mM) treatment for 24 h. Cells were collected, cell migration was determined by (A,B) Transwell assay, cell proliferation by (C) CCK-8 assay, and apoptosis by (D,E) annexin V-FITC/propidium iodide (PI) staining. Images were obtained under light microscopy (scale bar: 50 μm). The staining method for Transwell assay was crystal violet staining. Protein expression of E-cadherin, N-cadherin, vimentin, and MMP-9 was determined via Western blotting with density quantitative analysis (F-I) (n=4/group). Data are expressed as the mean ± standard deviation. *, P<0.05; **, P<0.01; ***, P<0.001. CCK-8, cell counting kit 8; EMT, epithelial-mesenchymal transition; GPIHBP1, glycosylphosphatidylinositol HDL-binding protein 1; MMP-9, Matrix metalloproteinase-9; NSCLC, non-small cell lung cancer; OE, overexpression.

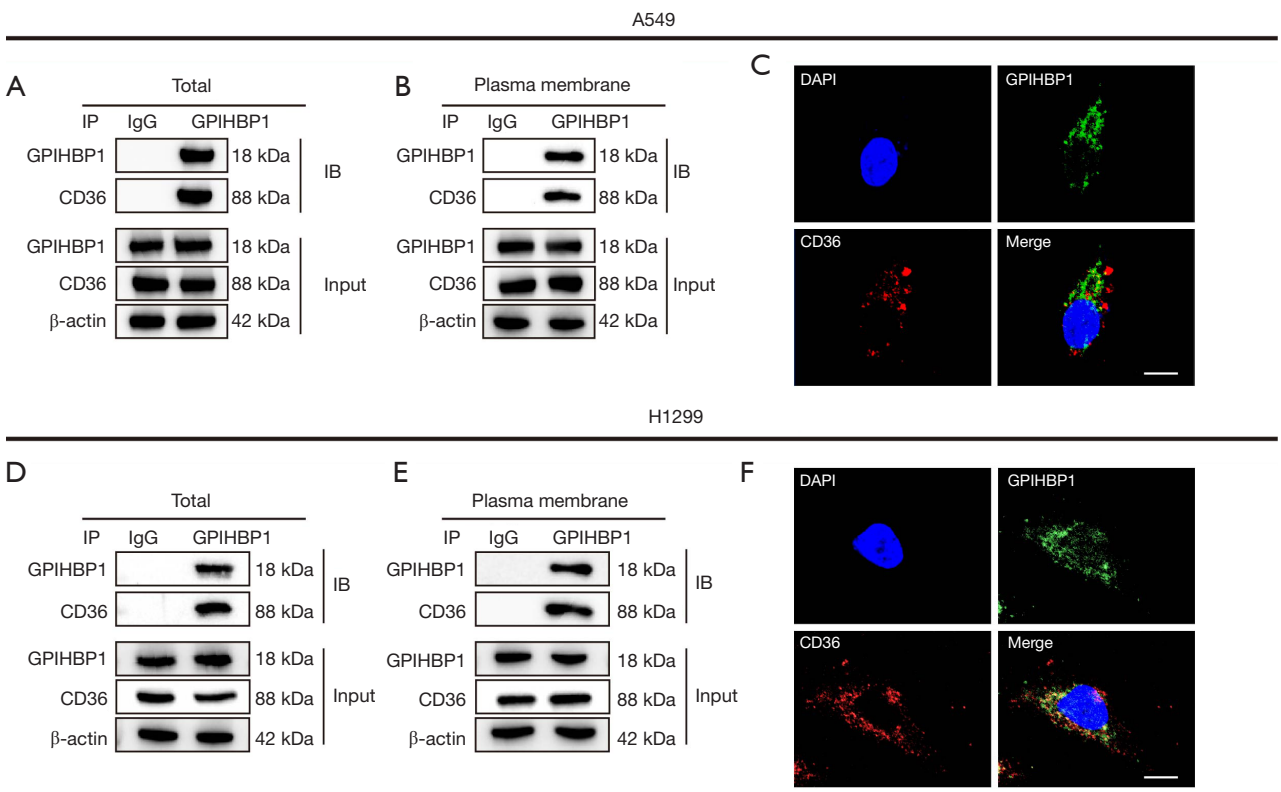

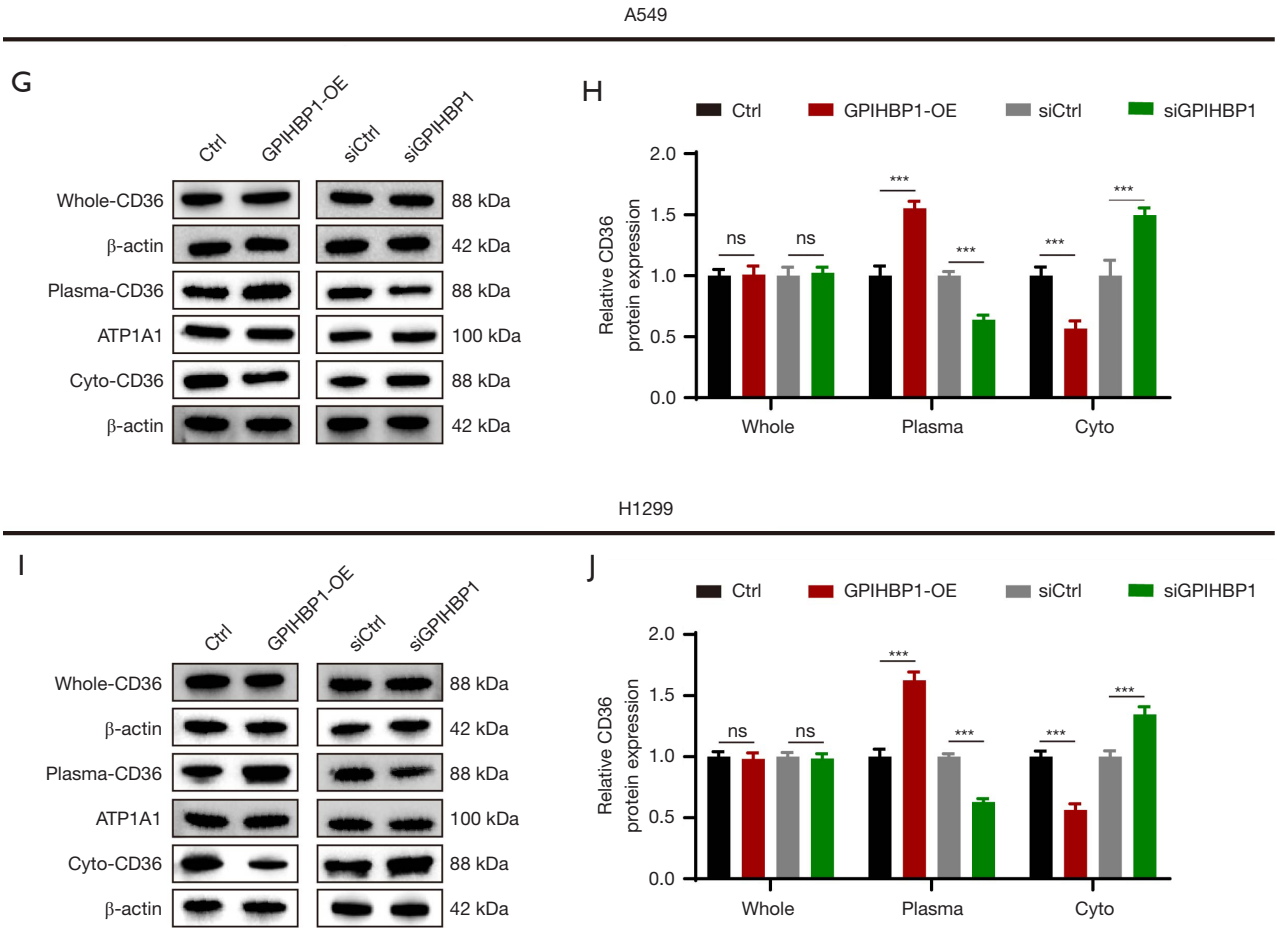

Figure 5 GPIHBP1 stabilized CD36 on the plasma membrane. (A-F) Co-IP and immunoblot analysis of the interaction between GPIHBP1 and CD36 in the whole lysates and plasma membrane lysates of NSCLC cells (n=4/group). (C,F) Representative images of immunofluorescence staining for GPIHBP1 (green), CD36 (red) and DAPI (blue) staining in NSCLC cells. Scale bar: 20 μm. (G-J) The GPIHBP1 protein was overexpressed by constructed lentiviral transfection or knocked down by small interfering RNA in NSCLC cells, and Western blotting and quantification of CD36 expression in the whole, plasma membrane, and cytosolic lysates in NSCLC cells were performed (n=4/group). Data are shown as the mean ± standard deviation. ***, P<0.001. CO-IP, co-inmunoprecipitation; DAPI, 4',6-diamidino-2-phenylindole); GPIHBP1, glycosylphosphatidylinositol HDL-binding protein 1; ns, no significant difference; NSCLC, non-small cell lung cancer; OE, overexpression.

an increased proportion of apoptotic cells (*Figure 6H,6I*). Overall, the exacerbating effects of GPIHBP1 knockdown on tumor progression were partly dependent on the expression of CD36.

GPIHBP1 overexpression inhibited NSCLC growth and metastasis in vivo

To examine the role of GPIHBP1 in lung cancer growth and metastasis *in vivo*, we established a xenograft model by transplanting luciferase-labeled control A549 or GPIHBP1-overexpressed A549 cells subcutaneously into nude mice. As shown in *Figure 7A,7B*, the IVIS spectrum demonstrated that the overexpression of GPIHBP1 significantly decreased the intensity of bioluminescent signals compared with those of the control group. Moreover, the tumor volume and tumor weight derived from GPIHBP1-overexpressed cells transplanted into nude mice were significantly smaller than those of control cells transplanted into nude mice (*Figure 7C-7E*). To determine the effect of GPIHBP1 overexpression on NSCLC cell metastasis, the mice were killed 30 days after injection of control and GPIHBP1

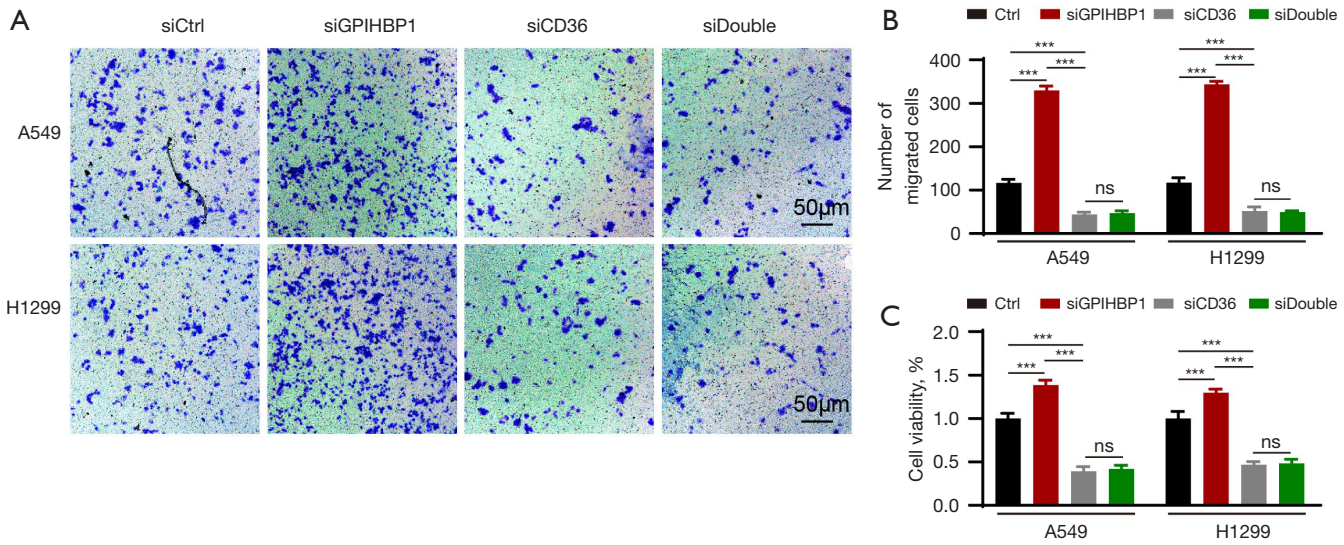

A549

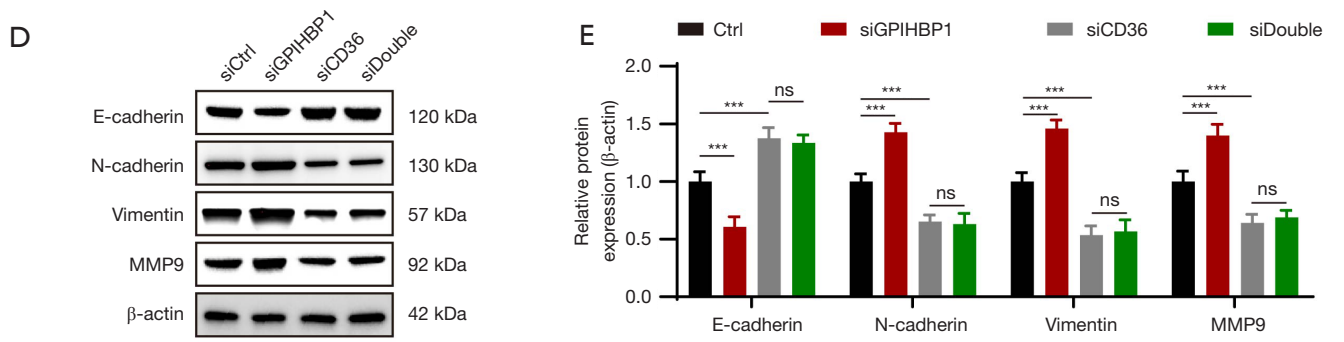

H1299

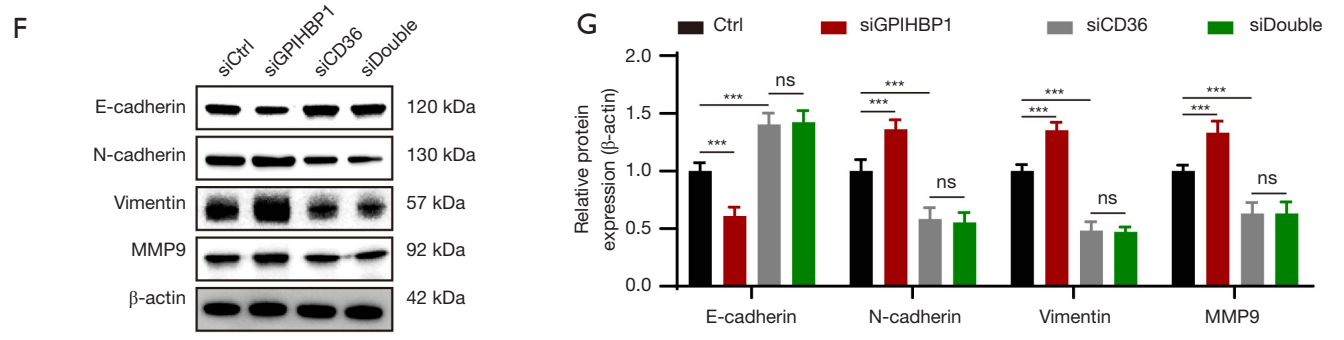

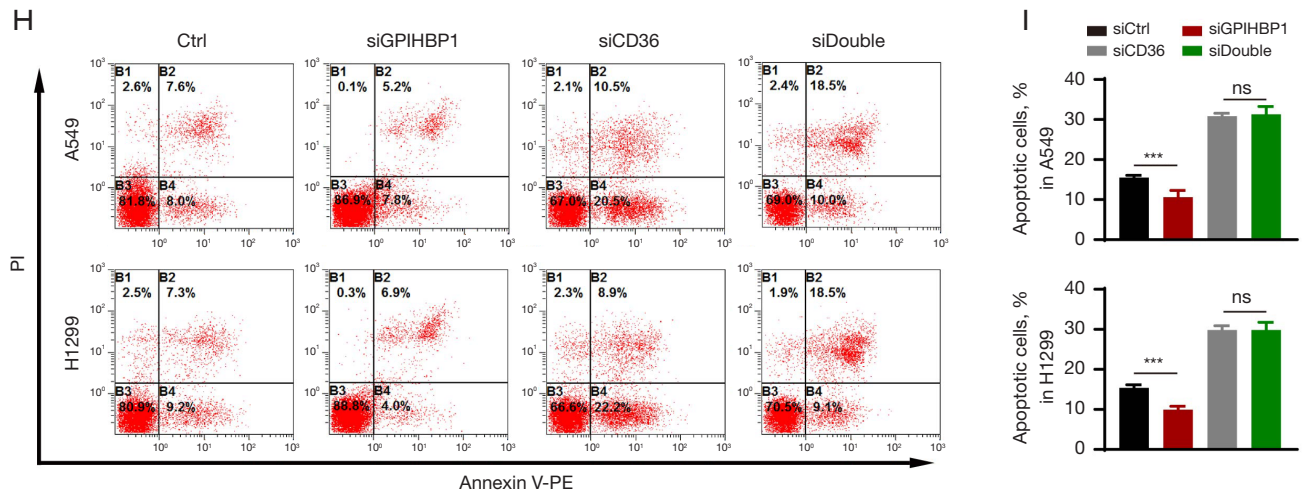

Figure 6 The procancer effects of GPIHBP1 knockdown were negated by downregulation of CD36. (A-I) In NSCLC cells, the GPIHBP1 protein or the CD36 were knocked down by small interfering RNA. Cells were collected for determination of cell proliferation and migration as detected as by (A,B) Transwell assay and for cell viability by (C) CCK-8 assay. Images were taken under light microscopy (scale bar: 50 μm). The staining method for Transwell assay was crystal violet staining. Protein expression of E-cadherin, N-cadherin, vimentin, and MMP-9 was determined by Western blotting with density quantitative analysis (D-G). Apoptosis was detected by annexin V-FITC/propidium iodide (PI) staining (H,I) (n=4/group). Data are expressed as the mean ± standard deviation. ***, P<0.001. CCK-8, cell counting kit 9; GPIHBP1, glycosylphosphatidylinositol HDL-binding protein 1; MMP-9, Matrix metalloproteinase-9; ns, no significant difference; NSCLC, non-small cell lung cancer.

overexpressing A549 cells through the tail vein. And the lung sections were subjected to HE staining. This indicated that NSCLC cell metastasis in mice with GPIHBP1 overexpression was decreased compared to that in mice of the control group (*Figure 7F*,*7G*). In summary, these data suggest that GPIHBP1 overexpression inhibited lung cancer growth and metastasis.

Discussion

Our study showed that aspirin inhibits cell proliferation and migration in NSCLC cells. Furthermore, long-term regular aspirin use can significantly reduce the overall risk of lung cancer. Moreover, we report, for the first time, that GPIHBP1 is downregulated in lung cancer but can be increased by aspirin. GPIHBP1 overexpression significantly inhibited cell proliferation or tumor progression in NSCLC cells. In addition, the inhibitory effects of aspirin on tumor progression were impaired by GPIHBP1 knockdown. Specifically, GPIHBP1 interacted with CD36 and stabilized CD36 on the plasma membrane. The procancer effect caused by GPIHBP1 knockdown was blocked by CD36 knockdown. Finally, our study demonstrated that GPIHBP1 overexpression inhibited lung cancer growth and metastasis *in vivo*. Taken together, these findings suggest that GPIHBP plays a suppressive role in lung cancer and that targeting GPIHBP may represent a new approach for treating lung cancer, as shown in *Figure 8*.

The prevalence of lung cancer has been rapidly increasing, and NSCLC is a major threat to human health worldwide (27). However, the underlying pathological mechanism of NSCLC remains unclear. As a nonselective Cox inhibitor, aspirin has been used clinically for more than 100 years (28). In addition to antipyretic and antiplatelet aggregation, among other effects, aspirin can also reduce the risk of a variety of cancers including digestive system tumors, breast cancer, and urinary system tumors (29-33). However, the underlying mechanism by which aspirin exerts its antitumor effects in NSCLC has not been fully explored. In this study, we first verified that aspirin could significantly inhibit the malignant behavior of NSCLC cells. Aspirin has significant suppressive effects on cell proliferation and migration in both A549 and H1299 cells. Moreover, by combining plasma exosome RNA-sequencing analysis in patients with or without aspirin treatment via bioinformation technology, we identified GPIHBP1

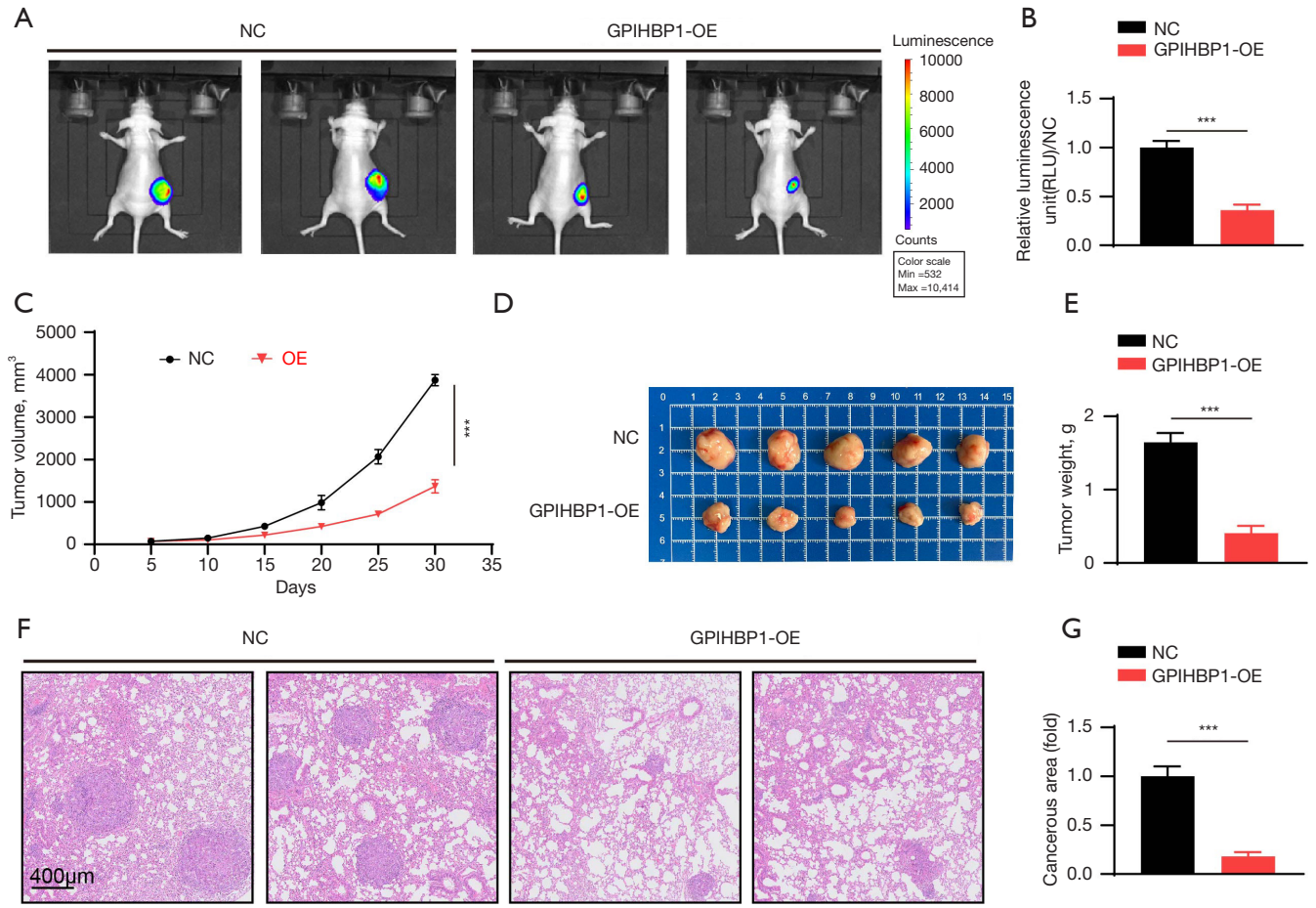

Figure 7 Overexpression of GPIHBP1 inhibited the xenograft tumor growth and metastasis of NSCLC cells *in vivo*. The nude mice were subcutaneously transplanted with A549 NC and A549 GPIHBP1-overexpression cells. (A,B) The tumor was collected 4 weeks later, and the size of tumor was measured. Representative bioluminescent images and quantification of bioluminescent imaging signal intensities were performed over 4 weeks (n=5/group). (C) The tumor volume was recorded once every 5 days. (D,E) Gross view and the weight of tumor samples were measured over 4 weeks (n=5/group). (F,G) Detection of metastatic nodules on lungs. After injection of control and GPIHBP1 overexpressing A549 cells through the tail vein, the mice were fed for another 30 days and then killed. Representative images were obtained of the macroscopic appearance and hematoxylin and eosin staining of lungs in nude mice, and the number of (G) metastatic tumors in the lungs of mice were counted (n=5/group). Scale bar, 400 μm. Data are expressed as the mean ± standard deviation. ***, P<0.001. GPIHBP1, glycosylphosphatidylinositol HDL-binding protein 1; NC, negative control; NSCLC, non-small cell lung cancer; OE, overexpression.

as a significant differentially expressed molecule. RNA-sequencing analysis showed that GPIHBP1 was upregulated after aspirin treatment. Furthermore, compared with adjacent the normal lung tissue, GPIHBP1 in lung tumor tissue was significantly decreased in patients with NSCLC. Hence, our study suggests that aspirin inhibits NSCLC cell proliferation and metastasis in a GPIHBP1-dependent manner.

As an essential component of LDL, GPIHBP1 captures LPL in the subendothelial spaces and then shuttles it to the capillary lumen (34,35). In a previous study, GPIHBP1-deficient (*Gpihbp1*$^{-/-}$) mice developed severe chylomicronemia under a chow diet due to the retention of LPL in the interstitial space (36). Interestingly, GPIHBP1 is abundant in the capillaries of the lung while LPL expression is low (37). The physiologic importance of GPIHBP1 in lung tissues is unclear. In the field of tumor-related research, it has been shown that GPIHBP1 is significantly associated with the progression of colorectal cancer (38). The effects of GPIHBP1 on NSCLC progression

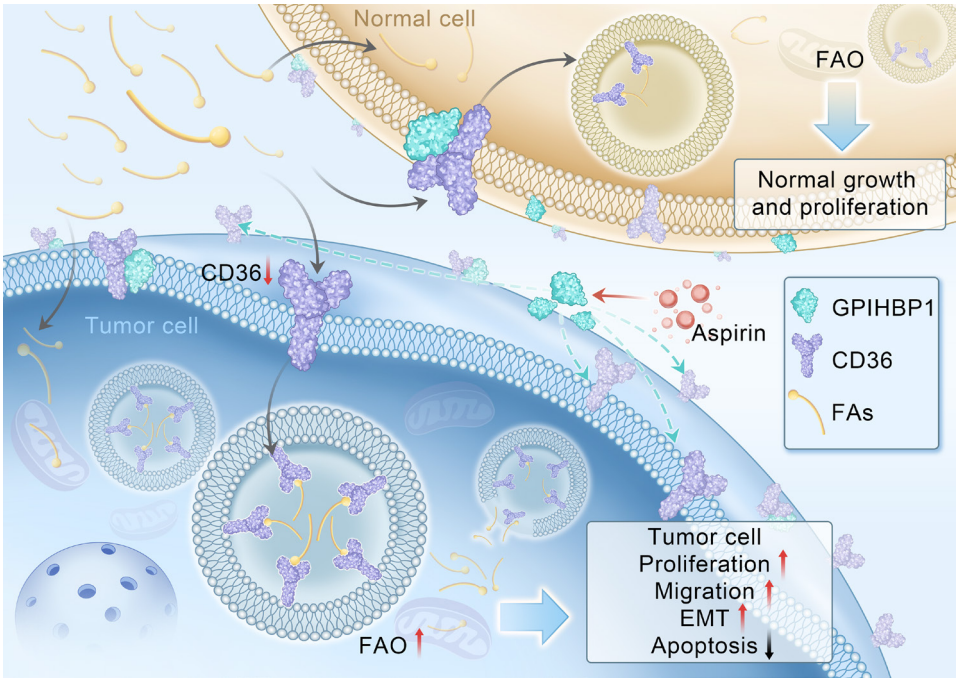

Figure 8 Schematic illustration of a novel molecular mechanism by which aspirin suppresses lung cancer development in a GPIHBP1-dependent manner. Aspirin can inhibit the malignant biological behavior of NSCLC by enhancing the expression of GPIHBP1. GPIHBP1 directly interacts with CD36 and that GPIHBP1 knockdown disrupts CD36 localization, which promotes tumor progression and metastasis in NSCLC. EMT, epithelial-mesenchymal transition; FAs, fatty acids; FAO, fatty acid oxidation; GPIHBP1, glycosylphosphatidylinositol HDL-binding protein 1; NSCLC, non-small cell lung cancer.

remains unknown. In our study, we found that GPIHBP1 overexpression inhibited migration, cell proliferation, and EMT but promoted apoptosis in NSCLC cells; meanwhile, the opposite was observed in GPIHBP1-knockdown cells. Our results indicated that GPIHBP1 inhibited NSCLC progression and metastasis. Furthermore, the inhibition of aspirin on tumor progression was largely negated by GPIHBP1 knockdown in both A549 cells and H1299 cells. Overall, we demonstrated the suppression of tumor progression by aspirin might also be mediated by regulating the GPIHBP1 expression in NSCLC.

We further explored the molecular mechanism by which GPIHBP1 regulates tumor progression. CD36 is a membrane protein belonging to the class B scavenger receptor family, mediating the endocytosis of fatty acids into cells (17). It has been reported that $CD36^{+}$ cancer cells exhibit increased fatty acid uptake, promoting their proliferation, migration, and EMT, making them more invasive and thus displaying stronger stem cell characteristics (39). Additionally, NSCLC cells, in order to meet the energy demands of their own biological malignant behaviors, shape and manipulate a complex tumor microenvironment, accompanied by rapid proliferation of capillaries in lung cancer tissues, resulting in abnormally active lipid metabolism in the lungs (40). High lipid levels, in turn, promote the expression of CD36, facilitating the occurrence and development of NSCLC (41). CD36 plays a pivotal function in the lipid metabolism (17,42,43). An increasing number of studies are reporting that CD36 overexpression promotes tumor development, metastasis, and drug resistance in various cancers (16,44-46). CD36 inhibition can reduce NSCLC development through regulating the AKT/mTOR pathway (41), and CD36 can translocate from plasma membrane to the cytoplasm to promote mitochondrial fatty-acid oxidation (FAO), which accelerates tumor growth and metastasis (47).

The co-immunoprecipitation results in our study indicated that GPIHBP1 could bind to CD36. Specifically, the downregulation of GPIHBP1 caused a deficiency of CD36 expression on the plasma membrane and upregulated CD36 expression in the cytoplasm. Importantly, the exacerbating effects of GPIHBP1 knockdown on tumor

progression were impaired by CD36 knockdown. These results indicated that GPIHBP1 stabilizes CD36 on the plasma membrane to maintain normal cell proliferation and migration. Therefore, a therapeutic strategy targeting CD36 and GPIHBP1 may exert effective inhibitory effects on NSCLC growth and metastasis.

Conclusions

Our study provides strong *in vitro* and *in vivo* evidence that aspirin can inhibit lung cancer progression and metastasis in a GPIHBP1-dependent manner. Additionally, we identified that GPIHBP1 directly interacts with CD36 and that GPIHBP1 knockdown disrupts CD36 localization, which promotes tumor progression and metastasis in NSCLC. Our findings point to a promising therapeutic strategy for the prevention and treatment of lung cancer.

Acknowledgments

We would like to thank Professor Yi Ru for guiding the design of this experiment and Zhongping Gu for his suggestions of revisions to the article.

Footnote

Reporting Checklist: The authors have completed the ARRIVE and MDAR reporting checklists. Available at https://tlcr.amegroups.com/article/view/10.21037/tlcr-2024-1174/rc

Data Sharing Statement: Available at https://tlcr.amegroups.com/article/view/10.21037/tlcr-2024-1174/dss

Peer Review File: Available at https://tlcr.amegroups.com/article/view/10.21037/tlcr-2024-1174/prf

Funding: The financial support for this investigation was granted by the Shaanxi Provincial Key R&D Program Projects (No. 2017ZDXM-SF-026), the Xi'an Science and Technology Program (No. 2023JH-YXYB-0320), and the Youth Innovation Project of Tangdu Hospital (No. 2023CTDQN029).

Conflicts of Interest: All authors have completed the ICMJE uniform disclosure form (available at https://tlcr.amegroups.com/article/view/10.21037/tlcr-2024-1174/coif). The authors have no conflicts of interest to declare.

Ethical Statement: The authors are accountable for all aspects of the work in ensuring that questions related to the accuracy or integrity of any part of the work are appropriately investigated and resolved. Written informed consents were obtained from each patient. The study protocol was performed in full accordance with the principles of the Declaration of Helsinki (as revised in 2013) and was approved by the Ethical Review Board of Tangdu Hospital (No. K202104-09). The protocol for animal experimentation in this study was approved by the Ethics Committee on Animal Experiments of Air Force Military Medical University (No. IACUC-20231251). All the animal experiments were carried out in accordance with the Guide for the Care and Use of Laboratory Animals (8th edition) published by the US National Institutes of Health.

References

1. Pan K, Concannon K, Li J, et al. Emerging therapeutics and evolving assessment criteria for intracranial metastases in patients with oncogene-driven non-small-cell lung cancer. Nat Rev Clin Oncol 2023;20:716-32.
2. Lee JM, McNamee CJ, Toloza E, et al. Neoadjuvant Targeted Therapy in Resectable NSCLC: Current and Future Perspectives. J Thorac Oncol 2023;18:1458-77.
3. Herbst RS, Morgensztern D, Boshoff C. The biology and management of non-small cell lung cancer. Nature 2018;553:446-54.
4. Wang M, Herbst RS, Boshoff C. Toward personalized treatment approaches for non-small-cell lung cancer. Nat Med 2021;27:1345-56.
5. Lanas A. Aspirin, cancer, and bleeding: an equation to solve. Lancet Gastroenterol Hepatol 2019;4:815-6.
6. Drew DA, Cao Y, Chan AT. Aspirin and colorectal cancer: the promise of precision chemoprevention. Nat Rev Cancer 2016;16:173-86.
7. Guo CG, Ma W, Drew DA, et al. Aspirin Use and Risk of Colorectal Cancer Among Older Adults. JAMA Oncol

2021;7:428-35.
8. Lichtenberger LM. Using aspirin to prevent and treat cancer. Inflammopharmacology 2024;32:903-8.
9. Hu X, Wu LW, Weng X, et al. Synergistic antitumor activity of aspirin and erlotinib: Inhibition of p38 enhanced aspirin plus erlotinib-induced suppression of metastasis and promoted cancer cell apoptosis. Oncol Lett 2018;16:2715-24.
10. Zhang X, Chen J, Cheng C, et al. Aspirin potentiates celecoxib-induced growth inhibition and apoptosis in human non-small cell lung cancer by targeting GRP78 activity. Ther Adv Med Oncol 2020;12:1758835920947976.
11. Liu Y, Yuan X, Li W, et al. Aspirin-triggered resolvin D1 inhibits TGF-β1-induced EMT through the inhibition of the mTOR pathway by reducing the expression of PKM2 and is closely linked to oxidative stress. Int J Mol Med 2016;38:1235-42.
12. Young SG, Fong LG, Beigneux AP, et al. GPIHBP1 and Lipoprotein Lipase, Partners in Plasma Triglyceride Metabolism. Cell Metab 2019;30:51-65.
13. Beigneux AP, Miyashita K, Ploug M, et al. Autoantibodies against GPIHBP1 as a Cause of Hypertriglyceridemia. N Engl J Med 2017;376:1647-58.
14. Young SG, Song W, Yang Y, et al. A protein of capillary endothelial cells, GPIHBP1, is crucial for plasma triglyceride metabolism. Proc Natl Acad Sci U S A 2022;119:e2211136119.
15. Goulbourne CN, Gin P, Tatar A, et al. The GPIHBP1-LPL complex is responsible for the margination of triglyceride-rich lipoproteins in capillaries. Cell Metab 2014;19:849-60.
16. Zhou X, Su M, Lu J, et al. CD36: The Bridge between Lipids and Tumors. Molecules 2024;29:531.
17. Guerrero-Rodríguez SL, Mata-Cruz C, Pérez-Tapia SM, et al. Role of CD36 in cancer progression, stemness, and targeting. Front Cell Dev Biol 2022;10:1079076.
18. Wang C, Yang Z, Xu E, et al. Apolipoprotein C-II induces EMT to promote gastric cancer peritoneal metastasis via PI3K/AKT/mTOR pathway. Clin Transl Med 2021;11:e522.
19. Mu N, Wang Y, Li X, et al. Crotonylated BEX2 interacts with NDP52 and enhances mitophagy to modulate chemotherapeutic agent-induced apoptosis in non-small-cell lung cancer cells. Cell Death Dis 2023;14:645.
20. Kuerban K, Gao X, Zhang H, et al. Doxorubicin-loaded bacterial outer-membrane vesicles exert enhanced anti-tumor efficacy in non-small-cell lung cancer. Acta Pharm Sin B 2020;10:1534-48.
21. Ren G, Ma Y, Wang X, et al. Aspirin blocks AMPK/SIRT3-mediated glycolysis to inhibit NSCLC cell proliferation. Eur J Pharmacol 2022;932:175208.
22. Zhao S, Mi Y, Guan B, et al. Tumor-derived exosomal miR-934 induces macrophage M2 polarization to promote liver metastasis of colorectal cancer. J Hematol Oncol 2020;13:156.
23. Xu Z, Chen Y, Ma L, et al. Role of exosomal non-coding RNAs from tumor cells and tumor-associated macrophages in the tumor microenvironment. Mol Ther 2022;30:3133-54.
24. He L, Zhu W, Chen Q, et al. Ovarian cancer cell-secreted exosomal miR-205 promotes metastasis by inducing angiogenesis. Theranostics 2019;9:8206-20.
25. Hu X, Matsumoto K, Jung RS, et al. GPIHBP1 expression in gliomas promotes utilization of lipoprotein-derived nutrients. Elife 2019;8:e47178.
26. Yang Y, Liu X, Yang D, et al. Interplay of CD36, autophagy, and lipid metabolism: insights into cancer progression. Metabolism 2024;155:155905.
27. Alduais Y, Zhang H, Fan F, et al. Non-small cell lung cancer (NSCLC): A review of risk factors, diagnosis, and treatment. Medicine (Baltimore) 2023;102:e32899.
28. Kang J, Jeong SM, Shin DW, et al. The Associations of Aspirin, Statins, and Metformin With Lung Cancer Risk and Related Mortality: A Time-Dependent Analysis of Population-Based Nationally Representative Data. J Thorac Oncol 2021;16:76-88.
29. Chan AT. Aspirin and the USPSTF-What About Cancer? JAMA Oncol 2022;8:1392-4.
30. Chen H, Qi Q, Wu N, et al. Aspirin promotes RSL3-induced ferroptosis by suppressing mTOR/SREBP-1/SCD1-mediated lipogenesis in PIK3CA-mutant colorectal cancer. Redox Biol 2022;55:102426.
31. Dehmer SP, O'Keefe LR, Evans CV, et al. Aspirin Use to Prevent Cardiovascular Disease and Colorectal Cancer: Updated Modeling Study for the US Preventive Services Task Force. JAMA 2022;327:1598-607.
32. Umar A, Loomans-Kropp HA. Role of Aspirin in Gastric Cancer Prevention. Cancer Prev Res (Phila) 2022;15:213-5.
33. Yaghjyan L, Eliassen AH, Colditz G, et al. Associations of aspirin and other anti-inflammatory medications with breast cancer risk by the status of COX-2 expression. Breast Cancer Res 2022;24:89.
34. Jiang S, Ren Z, Yang Y, et al. The GPIHBP1-LPL complex and its role in plasma triglyceride metabolism:

Insights into chylomicronemia. Biomed Pharmacother 2023;169:115874.
35. Liu C, Li L, Guo D, et al. Lipoprotein lipase transporter GPIHBP1 and triglyceride-rich lipoprotein metabolism. Clin Chim Acta 2018;487:33-40.
36. Liu X, Li J, Liao J, et al. Gpihbp1 deficiency accelerates atherosclerosis and plaque instability in diabetic Ldlr(-/-) mice. Atherosclerosis 2019;282:100-9.
37. Beigneux AP, Davies BS, Bensadoun A, et al. GPIHBP1, a GPI-anchored protein required for the lipolytic processing of triglyceride-rich lipoproteins. J Lipid Res 2009;50 Suppl:S57-62.
38. Gao M, Liao L, Lin Z, et al. Increase in GPIHBP1 expression in advanced stage colorectal cancer indicates poor immune surveillance. Transl Cancer Res 2024;13:2691-703.
39. Xia L, Zhou Z, Chen X, et al. Ligand-dependent CD36 functions in cancer progression, metastasis, immune response, and drug resistance. Biomed Pharmacother 2023;168:115834.
40. Ao YQ, Gao J, Zhang LX, et al. Tumor-infiltrating CD36(+)CD8(+)T cells determine exhausted tumor microenvironment and correlate with inferior response to chemotherapy in non-small cell lung cancer. BMC Cancer 2023;23:367.
41. Liu H, Guo W, Wang T, et al. CD36 inhibition reduces non-small-cell lung cancer development through AKT-mTOR pathway. Cell Biol Toxicol 2024;40:10.
42. Ruan C, Meng Y, Song H. CD36: an emerging therapeutic target for cancer and its molecular mechanisms. J Cancer Res Clin Oncol 2022;148:1551-8.
43. Glatz JFC, Heather LC, Luiken J. CD36 as a gatekeeper of myocardial lipid metabolism and therapeutic target for metabolic disease. Physiol Rev 2024;104:727-64.
44. Luo X, Zheng E, Wei L, et al. The fatty acid receptor CD36 promotes HCC progression through activating Src/PI3K/AKT axis-dependent aerobic glycolysis. Cell Death Dis 2021;12:328.
45. Zhang J, Li X, Yang J, et al. MiR-1254 suppresses the proliferation and invasion of cervical cancer cells by modulating CD36. J Transl Med 2022;19:531.
46. Drury J, Rychahou PG, Kelson CO, et al. Upregulation of CD36, a Fatty Acid Translocase, Promotes Colorectal Cancer Metastasis by Increasing MMP28 and Decreasing E-Cadherin Expression. Cancers (Basel) 2022;14:252.
47. Wang H, Franco F, Tsui YC, et al. CD36-mediated metabolic adaptation supports regulatory T cell survival and function in tumors. Nat Immunol 2020;21:298-308.

Cite this article as: Liu W, Qiao D, Chen J, Gao Y, Okuda K, Shimada Y, Yao L. Aspirin impedes non-small cell lung cancer development via fine-tuning the CD36 localization regulated by GPIHBP1. Transl Lung Cancer Res 2025;14(2):491-512. doi: 10.21037/tlcr-2024-1174